Hydrogenic impurity in a parabolic quantum wire in a magnetic field: Quantum chaos and optical properties

Pawel Hawrylak
Institute for Microstructural Sciences, National Research Council of Canada, Ottawa, Canada K1A OR6

Marek Grabowski
Department of Physics, University of Colorado, Colorado Springs, Colorado 80933
(Received 8 October 1993)

We investigate electronic states and the far-infrared absorption spectrum of a two-dimensional (2D) hydrogenic impurity in a parabolic quantum wire in a magnetic field. The problem is mapped into the problem of interacting nonlinear harmonic oscillators. The evolution of the energy levels and level statistics from a 2D to a 1D effective hydrogen atom is investigated in the quantum and classically chaotic regimes. The ground-state energy reflects a delicate balance between a blueshift due to confinement and a redshift due to an increase in binding energy. In the absence of a magnetic field, the model reduces to the well-known problem of quantum chaos in a 3D hydrogen atom in a magnetic field in a zero angular-momentum channel. The presence of a magnetic field in the wire breaks the scaling behavior inherent in the 3D hydrogen problem.

INTRODUCTION

There is currently a great deal of interest in the optical properties of low-dimensional structures.[1-4] Far-infrared (FIR) optical properties are often determined by impurity transitions while interband optics involves bound electron-valence hole pairs. Both processes require the solution of the effective hydrogenic-impurity problem. In this paper, we study the problem of a two-dimensional (2D) hydrogen impurity in a parabolic quantum wire in the presence of a magnetic field normal to the plane. This model represents the simplest generic system available to study donors and localized excitons in quantum wires. It allows us to investigate the evolution from a quasi-two-dimensional to a quasi-one-dimensional atom as a function of the strength of the confining potential. This evolution is nontrivial due to the infinite binding energy of a 1D hydrogen atom.[5] We shall also demonstrate that as a result of the 1D confining potential, the underlying classical dynamics of an electron becomes chaotic. This makes the computation and the interpretation of the energy spectrum nontrivial.

There is currently a great deal of interest in the quantum properties of systems with underlying chaotic classical dynamics. Much of the progress in the current understanding of the relationship between classical and quantum chaos comes from studying experimental systems. A very good example is the optical spectrum of a hydrogen atom in a magnetic field.[6] In the 3D hydrogen problem, chaotic behavior arises because of the destruction by the magnetic field of a continuous rotational symmetry and associated with its constants of motion. Surprisingly, both experimental and theoretical progress have been achieved[6,7] only very recently. We show here that the hydrogenic impurity in quasi-two-dimensional parabolic wires provides an interesting experimental possibility to study quantum systems with chaotic classical dynamics. The chaotic behavior results from the destruction of the rotational symmetry by the confining potential.

THE MODEL

Let us consider the electronic states and absorption spectrum of a hydrogen atom confined in a two-dimensional[8] parabolic quantum wire. The positively charged center represents either a localized photoexcited valence hole or a donor impurity. The magnetic field is applied perpendicular to the plane of the wire.

The Hamiltonian for a single electron with mass m moving in the (x,y) plane in the field of an attractive Coulomb potential and in a magnetic field B in the z direction is given in symmetrical gauge by

$$H=\frac{1}{2m}\left[p_x-\frac{eB}{2c}y\right]^2+\frac{1}{2m}\left[p_y+\frac{eB}{2c}x\right]^2 -\frac{e^2}{\varepsilon|\mathbf{r}|}+\tfrac{1}{8}m\omega_y^2y^2 . \quad (1)$$

Here $e^2/\varepsilon|\mathbf{r}|$ is the attractive potential of the donor (hole), ε is the background dielectric constant, $m\omega_y^2y^2/8$ is the parabolic confining potential in the y direction, and we take $\hbar=1$. Measuring lengths in terms of the effective Bohr radius a_0 and energy in terms of the effective Ry we can write the dimensionless Schrödinger equation for the wave function $f(x,y)$ as

$$\left[\frac{p_x^2+p_y^2}{2}+\frac{\gamma}{2}L_z+\tfrac{1}{8}\gamma^2(x^2+y^2)+\tfrac{1}{8}\beta^2y^2-\frac{1}{\sqrt{x^2+y^2}}\right] \times f(x,y)=\frac{E}{2}f(x,y) , \quad (2)$$

with $L_z=xp_y-yp_x$ being the z component of the angular momentum. The parameter $\gamma=\omega_c/2$ Ry and parameter $\beta=\omega_y/2$ Ry measures the strength of the magnetic field

($\omega_c = eB/mc$) and the strength of the confining potential with respect to the Coulomb potential ($\mathrm{Ry} = e^2/2\varepsilon a_0$). In typical semiconductor nanostructures, γ and β are typically between 0 and 1.

In the absence of an impurity, Eq. (2) describes a superposition of free motion in the x direction and a harmonic motion with energy spacing β in the γ direction.

In the absence of the parabolic confinement, Eq. (2) describes the 2D hydrogen atom in the magnetic field. Its energy spectrum and eigenstates have been studied by a number of authors.[8] Because there are two conserved quantities, energy E and angular momentum L_z, the Hamiltonian of the 2D hydrogen atom in a magnetic field is fully integrable, and hence exactly soluble. The wave functions and energies can be obtained by a variety of well-defined methods. The confinement, on the other hand, destroys the circular symmetry, and angular momentum L_z is no longer an integral of motion. This lack of a conserved quantity, coupled with a highly nonlinear form of the total confining potential, leads to chaotic dynamics in the classical problem.

It is a standard procedure to remove the divergence of the Coulomb potential by a transformation from rectangular coordinates (x,y) into parabolic coordinates (u,v), or alternatively, from cylindrical coordinates (ρ,Φ) into parabolic cylindrical coordinates (μ,ϕ):

$$\{x=\tfrac{1}{2}(u^2-v^2); y=uv\} \text{ or } \{\rho=\tfrac{1}{2}\mu^2; \Phi=2\phi\} . \tag{3}$$

The regularized Schrödinger equation in parabolic coordinates (u,v) can now be written as

$$\left[\frac{p_u^2+p_v^2}{2}-E\left[\frac{u^2+v^2}{2}\right]+\frac{\gamma}{2}\left[\frac{u^2+v^2}{2}\right]L_z+\frac{1}{4}\gamma^2\left[\frac{u^2+v^2}{2}\right]^3+\frac{1}{4}\beta^2\left[\frac{u^2+v^2}{2}\right]u^2v^2\right]f(u,v)=2f(u,v) . \tag{4}$$

Equation (4) can be interpreted as either a generalized eigenvalue problem for energy E or, given energy E, an eigenvalue problem for the charge of the hole. The left-hand side describes a Hamiltonian Q of a pair of coupled nonlinear harmonic oscillators with energy $(-E)$ playing the role of a force constant. The classical motion corresponds to orbits on a constant-charge ($Q=2$) surface. For zero magnetic field ($\gamma=0$), Eq. (4) reduces to the Schrödinger equation appropriate for a 3D hydrogen atom in a magnetic field in the zero angular-momentum channel.[7,9,10]

The regularized Hamiltonian Q can be written in parabolic cylindrical coordinates (μ,ϕ) as

$$Q=\frac{1}{2}p_\mu^2+\frac{1}{2\mu^2}p_\phi^2-\frac{\mu^2}{2}E+\frac{\gamma}{2}\frac{\mu^2}{2}p_\phi +\tfrac{1}{4}[\gamma^2+\beta^2\sin^2(2\phi)]\left[\frac{\mu^2}{2}\right]^3 . \tag{5}$$

Classical equations of motion describe the evolution of canonical variables (ϕ,p_ϕ) and (μ,p_μ) in effective time τ related to the real time t via $d\tau=dt/\mu^2$ on a surface of constant charge $Q=2$:

$$\begin{aligned} &\dot{p}_\phi=-\frac{\beta^2}{2}\left[\frac{\mu^2}{2}\right]^3\sin(4\phi) , \quad \dot{\phi}=\frac{p_\phi}{\mu^2}+\gamma\frac{\mu^2}{4} , \quad \dot{\mu}=p_\mu , \\ &p_\mu=\pm\left[4-\frac{1}{\mu^2}p_\phi^2+\mu^2E-\gamma\frac{\mu^2}{2}p_\phi -\tfrac{1}{2}[\gamma^2+\beta^2\sin^2(2\phi)]\left[\frac{\mu^2}{2}\right]^3\right]^{1/2} . \end{aligned} \tag{6}$$

For zero magnetic field ($\gamma=0$), the simplest periodic orbits correspond to $\phi=n(\pi/4)$ ($n=0,1,2,\ldots$), $\dot{\phi}=0$, $\dot{p}_\phi=0$, $p_\phi=0$. The $n=0$ orbit I_0 corresponds to motion along the direction of the wire while $n=1$ orbit I_1 corresponds to the direction perpendicular to the wire. It is easy to see from equations of motion that the $n=1$ orbit at the classical ionization threshold $E=0$ corresponds to the oscillatory motion of the electron with frequency ω proportional to β, $\omega=\kappa\beta$, i.e., the frequency of the free-particle motion in the y direction. The effect of impurity is present in the proportionality constant κ. This is an equivalent of the Garton-Tomkins frequency[11] in the 3D hydrogen atom, and we expect that both classical orbits will lead to the modulation of the photoabsorption spectrum. A full analysis of the classical motion and the effect of the magnetic field will be given elsewhere.[12]

It is illuminating to examine the *negative* energy spectrum ($E<0$) in the *zero magnetic field* case ($\gamma=0$). Let us define $E=-\omega^2$ and rescale our coordinates and momenta as $u\to u\sqrt{\omega}$ $p_u\to p_u/\sqrt{\omega}$. This allows us to rewrite Eq. (4) as

$$\left[\frac{p_u^2+p_v^2}{2}+\tfrac{1}{2}(u^2+v^2)+\tfrac{1}{8}\tilde{\beta}^2(u^2+v^2)u^2v^2\right]f(u,v) =2ef(u,v) , \tag{7}$$

where $\tilde{\beta}=\beta/\omega^2$ and $e=1/\omega$ are *scaled* coupling constant and eigenvalues. Because of scaling, Eq. (7) does not depend on energy and confinement separately, but only through a single-scaled variable. The application of the magnetic field in a wire destroys the scaling property. Equation (7) describes a pair of coupled nonlinear harmonic oscillators and has been studied by a number of authors.[7,9]

In an analogy to previous works,[7,9,10] we expand all operators in the basis of harmonic-oscillator states, i.e., in terms of a pair of harmonic oscillator lowering (raising) operators (d,b)

$$\begin{aligned} u&=(b+b^+ +d^+ +d)/2 , \\ v&=(b-b^+ +d^+ -d)/2i , \\ v^2&=H_0/2-(b^+d+d^+b)/2 \\ &\quad -\{(b-d)^2+(b^+-d^+)^2\}/4 , \end{aligned}$$

$$u^2=H_0/2+(b^+d+d^+b)/2$$
$$+\{(b-d)^2+(b^+-d^+)^2\}/4\ ,$$
$$L=d^+d-b^+b\ ,$$
$$u^2+v^2=H_0+(bd+b^+d^+)\ ,$$
$$p_u^2+p_v^2=H_0-(bd+b^+d^+)\ ,$$

where $H_0=d^+d+b^+b+1$ and the physically allowed values of the angular momentum are $L=0,\pm2,\pm4,\ldots$. Expanding the wave function $f(u,v)$ in terms of harmonic-oscillator states $f(u,v)=\sum_{n,m}a_{n,m}f_{n,m}(u,v)$ transforms Eqs. (4) and (7) into a matrix equation for coefficients $a_{n,m}$, which can be solved by standard methods. The resulting energy spectrum can be probed optically. We use dipole approximation for the coupling with radiation and consider two different absorption spectra $A_{x(y)}(E)$ corresponding to linear polarization along the x or y axis. The absorption spectrum is now given by $A_{x(y)}(E)=\sum_\alpha|M_{\alpha0}|^2\delta[E-(E_\alpha-E_0)]$ where dipole matrix elements $M_{\alpha0}$ for the transition from the ground-state 0 to the excited-state α can be easily calculated:

$$M_{\alpha0}\begin{bmatrix}x\\y\end{bmatrix}=\sum_{n,m,n',m',n'',m''}a^{\alpha*}_{nm}\langle nm|u^2+v^2|n'm'\rangle\left\langle n'm'\left|\begin{bmatrix}u^2-v^2\\uv\end{bmatrix}\right|n''m''\right\rangle a^0_{n''m''}\ . \tag{9}$$

RESULTS AND DISCUSSION

Because of the scaling properties for $\tilde{\beta}=0$, Eq. (7) is exactly soluble and gives immediately the energy spectrum of the 2D hydrogen atom: $E_{n,m}=4/(n+m+1)^2$ with $(n-m=\pm2p,\ p=0,1,2,\ldots)$, while unscaled Eq. (4) reproduces this exact result for sufficiently large basis set. Good convergence of low eigenvalues is achieved with several hundred oscillator states (200–400).

We study first the effect of confinement β on the energy spectrum using a truncated harmonic-oscillator basis in Eq. (4). Figure 1 shows the 50 lowest eigenvalues as a function of β in the absence of the magnetic field ($\gamma=0$). The inset shows a typical weak "diamagnetic" dependence of the ground-state energy on confinement energy β, i.e., $E_g\approx\beta^2$. We can simply understand this weak dependence of the ground-state energy on confinement as a result of the competion between the increase in kinetic energy (blueshift) and binding energy (redshift). At large confinement, the binding energy increases as $\beta^{1/2}$ with respect to the lowest subband energy $\beta/2$. The remaining spectrum shows increasing level spacing and level interaction associated with the removal of the rotational symmetry. The remaining degeneracies associated with the amplitude of the angular momentum are further removed by the application of the magnetic field. We show the evolution of the 50 lowest energy levels from $\beta=1.0$, $\gamma=0.0$ to $\beta=1.0$, $\gamma=1.0$ in Fig. 2. The spectrum becomes quite complicated with a large degree of level repulsion. In the inset, the diamagnetic shift of the ground state is shown. Both Figs. 1 and 2 illustrate the removal of degeneracies of the 2D hydrogen atom by the confining potential leading to level repulsion and a mean energy spacing $\langle dE\rangle$. In Fig. 3, we show the distribution of energy spacing dE in a lower part of the spectrum (200 out of 441) for zero confinement [Fig. 3(a)], $\beta=1.0$, $\gamma=0.0$ [Fig. 3(b)], and $\beta=1.0$, $\gamma=1.0$ [Fig. 3(c)]. The zero-confinement distribution [Fig. 3(a)] appears to follow

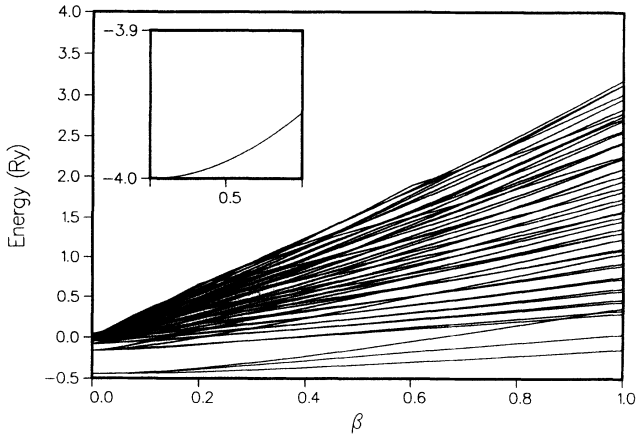

FIG. 1. Fifty (out of 441) lowest energy levels as a function of confinement strength β in the absence of the magnetic field ($\gamma=0$). The inset shows a typical weak diamagnetic dependence of the ground-state energy on confinement energy β.

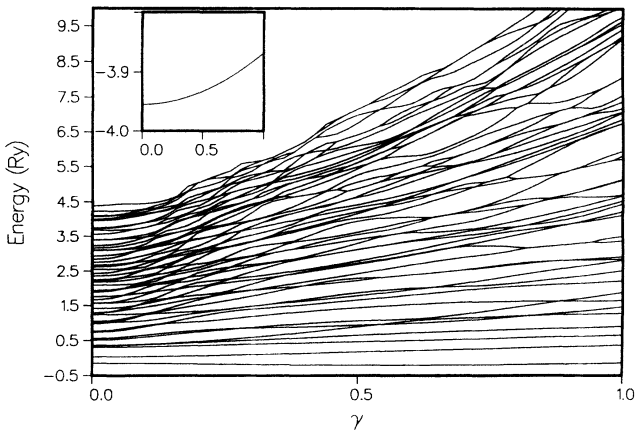

FIG. 2. Fifty (out of 225) lowest energy levels as a function of magnetic field γ for a wire with subband spacing $\beta=1$. The inset shows a typical weak diamagnetic dependence of the ground-state energy on magnetic field γ.

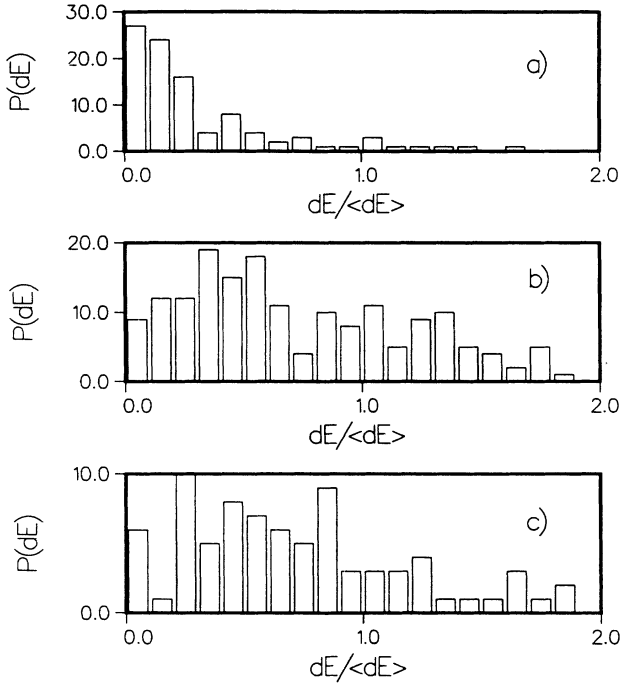

FIG. 3. Distributions $P(dE)$ (unnormalized) of normalized energy spacings $dE/\langle dE\rangle$ of lowest energy levels for (a) 2D ($\beta=0$, $\gamma=0$), (b) wire ($\beta=1$, $\gamma=0$), and (c) wire in a magnetic field ($\beta=1,\gamma=1$).

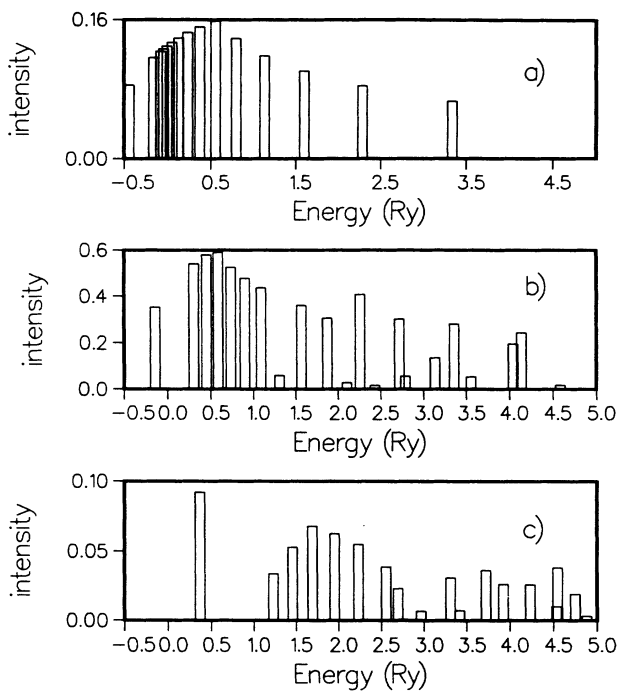

FIG. 4. (a) The reference spectrum of the 2D atom independent of the polarization of radiation for ($\beta=0$, $\gamma=0$), (b) x-polarized spectrum of the wire ($\beta=1$, $\gamma=0$), and (c) y-polarized spectrum of the wire ($\beta=1$, $\gamma=0$).

a Poisson distribution while finite-confinement spectra (with or without the magnetic field) appear to follow Wigner distribution, a characteristic feature of quantum systems with underlying chaotic classical dynamics.

Finally we turn to the effect of confinement on the FIR spectrum. The FIR spectrum in our truncated oscillator basis is shown in Fig. 4. Figure 4(a) shows the reference spectrum of the 2D atom independent of the polarization of radiation for ($\beta=0$, $\gamma=0$), while Fig. 4(b) shows the x-polarized spectrum of the wire ($\beta=1$, $\gamma=0$), and Fig. 4(c) shows the y-polarized spectrum of the wire ($\beta=1$, $\gamma=0$). The spectra of the wire are shifted toward higher energies due to confinement, with the shift for the y polarization being larger. This is understandable since it probes the strongly confined motion in the direction perpendicular to the wire. As expected, spectra at higher energy look quite ordered, with equally spaced peaks due to underlaying chaotic dynamics. The details of the spectrum are, however, still sensitive to the size of the basis, and more extensive numerical work is required.

In summary, we investigated the problem of a Coulombic impurity in the center of a parabolic wire in a magnetic field as a model of donors and excitons in quantum wires. We have shown that the effect of confinement leads to a complex problem with underlying chaotic classical dynamics. The effects of chaos are manifest in the spectrum of energy levels and in the FIR spectrum. The chaotic regime is also very important in low-energy transport through wires with impurities and in excitonic recombination in quantum wires.

ACKNOWLEDGMENT

We thank G. C. Aers for discussion. One of us (M.G.) thanks the Institute for Microstructural Sciences, NRC Canada, for hospitality and financial support.

[1]For a recent review see, *Optical Phenomena in Semiconductor Structures of Reduced Dimensions,* Vol. 248 of *NATO Advanced Study Institute, Series E,* edited by D. J. Lockwood and A. Pinczuk (Kluwer Academic, Dordrecht, 1993).

[2]A. S. Plaut, H. Lage, P. Grambow, D. Heitmann, K. von Klitzing, and K. Ploog, Phys. Rev. Lett. **67**, 1642 (1991).

[3]J. M. Calleja, A. R. Goni, B. S. Dennis, J. S. Weiner, A. Pinczuk, S. Schmitt-Rink, L. N. Pfeiffer, K. W. West, J. F. Mueller, and A. E. Ruckenstein, Solid State Commun. **79**, 911 (1991).

[4]G. W. Bryant, Phys. Rev. B **26**, 6632 (1984); M. Fritze, A. V. Nurmikko, and P. Hawrylak, *ibid.* **48**, 4960 (1993); P. Hawrylak, Solid State Commun. **81**, 525 (1992).

[5]R. Loudon, Am. J. Phys. **27**, 649 (1959).

[6]Chun-ho Iu, George R. Welch, Michael M. Kash, Daniel Kleppner, D. Delande, and J. C. Gay, Phys. Rev. Lett. **64**, 145 (1991).

[7]D. Delande and J. C. Gay, Phys. Rev. Lett. **57**, 2006 (1986); **57**, 141 (1991); D. Delande, A. Bommier, and J. C. Gay, *ibid.* **66**, 141 (1993).

[8]A. H. MacDonald and D. S. Ritchie, Phys. Rev. B **33**, 8336 (1985), and references therein.

[9]H. Hasegawa, M. Robnik, and G. Wunner, Prog. Theor. Phys. **98**, 198 (1989).

[10]Harald Friedrich and Dieter Wintgen, Phys. Rep. **183**, 37 (1989).

[11]W. R. S. Garton and F. S. Tomkins, Astrophys. J. **158**, 839 (1969).

[12]M. Grabowski and P. Hawrylak (unpublished).